Developmental Cell
Article

α-Actinin Is Required for Tightly Regulated Remodeling of the Actin Cortical Network during Cytokinesis

Svetlana Mukhina,[1] Yu-li Wang,[3] and Maki Murata-Hori[1,2,*]
[1]Mammalian Cell Biology Group, Temasek Life Sciences Laboratory
[2]Department of Biological Sciences
The National University of Singapore, 1 Research Link, 117604, Singapore
[3]Department of Physiology, University of Massachusetts Medical School, 377 Plantation Street, Worcester, MA 01605, USA
*Correspondence: makihori@tll.org.sg
DOI 10.1016/j.devcel.2007.08.003

SUMMARY

Localization of the actin crosslinking protein, α-actinin, to the cleavage furrow has been previously reported. However, its functions during cytokinesis remain poorly understood. We have analyzed the functions of α-actinin during cytokinesis by a combination of molecular manipulations and imaging-based techniques. α-actinin gradually dissipated from the cleavage furrow as cytokinesis progressed. Overexpression of α-actinin caused increased accumulation of actin filaments because of inhibition of actin turnover, leading to cytokinesis failure. Global depletion of α-actinin by siRNA caused a decrease in the density of actin filaments throughout the cell cortex, surprisingly inducing accelerated cytokinesis and ectopic furrows. Local ablation of α-actinin induced accelerated cytokinesis specifically at the site of irradiation. Neither overexpression nor depletion of α-actinin had an apparent effect on myosin II organization. We conclude that cytokinesis in mammalian cells requires tightly regulated remodeling of the cortical actin network mediated by α-actinin in coordination with actomyosin-based cortical contractions.

INTRODUCTION

Cytokinesis is a spatially and temporally regulated event crucial for accurate separation of chromosomes and organelles into two daughter cells. In animal cells, cortical ingression takes place along the equator after chromosome separation. In spite of recent advances, which have led to an increased understanding of division-plane positioning (Maddox and Oegema, 2003; Glotzer, 2004), it remains predominantly unknown how cortical ingression is regulated during cytokinesis. Because of the existence of strong cortical forces (Burton and Taylor, 1997), and the concentration of actin filaments and myosin II along the equator (Fujiwara and Pollard, 1976; Sanger and Sanger, 1980; Maupin and Pollard, 1986), it is widely believed that cortical ingression involves the constriction of an actomyosin contractile ring (Satterwhite and Pollard, 1992). However, the process appears to be more complex than the simple constriction of a contractile ring (Wang, 2005).

Several reports have shown that actin is highly dynamic along the equator (Pelham and Chang, 2002; Murthy and Wadsworth, 2005; Guha et al., 2005) and that both actin assembly and disassembly are required for cytokinesis (O'Connell et al., 2001; Pelham and Chang, 2002; Murthy and Wadsworth, 2005; Guha et al., 2005). In fission yeast, inhibition of actin polymerization by low doses of latrunculin A induced a decreased rate of ring closure (Pelham and Chang, 2002), suggesting that cytokinesis requires the integrity of certain actin structures. A similar phenotype was also observed after global application of latrunculin A to mammalian cells (Murthy and Wadsworth, 2005). On the other hand, local application of cytochalasin D or latrunculin A at the equator facilitates cytokinesis, suggesting that cortical actin disassembly promotes cytokinesis (O'Connell et al., 2001).

Recent studies suggested that myosin II activity plays a role in facilitating actin turnover along the equator (Murthy and Wadsworth, 2005; Guha et al., 2005). Actin depolymerizing factor (ADF)/cofilin is also likely to be involved in not only formation and maintenance of the contractile ring (Nakano and Mabuchi, 2006) but also the regulation of actin disassembly during furrow ingression, because its knockdown resulted in the robust accumulation of actin filaments along the equator and cytokinesis failure (Gunsalus et al., 1995; Somma et al., 2002; Hotulainen et al., 2005). In addition to actin assembly and disassembly, cytokinesis probably involves remodeling of a cortex-associated, crosslinked actin-filament network.

An actin crosslinking protein termed α-actinin was found in the cleavage furrow of animal cells almost 30 years ago (Fujiwara et al., 1978; Mabuchi et al., 1985; Sanger et al., 1987). α-actinin is a homodimer with two subunits of molecular mass ~100 kDa each (Suzuki et al., 1976) arranged in an antiparallel orientation (Djinovic-Carugo et al., 1999; Ylanne et al., 2001). It is

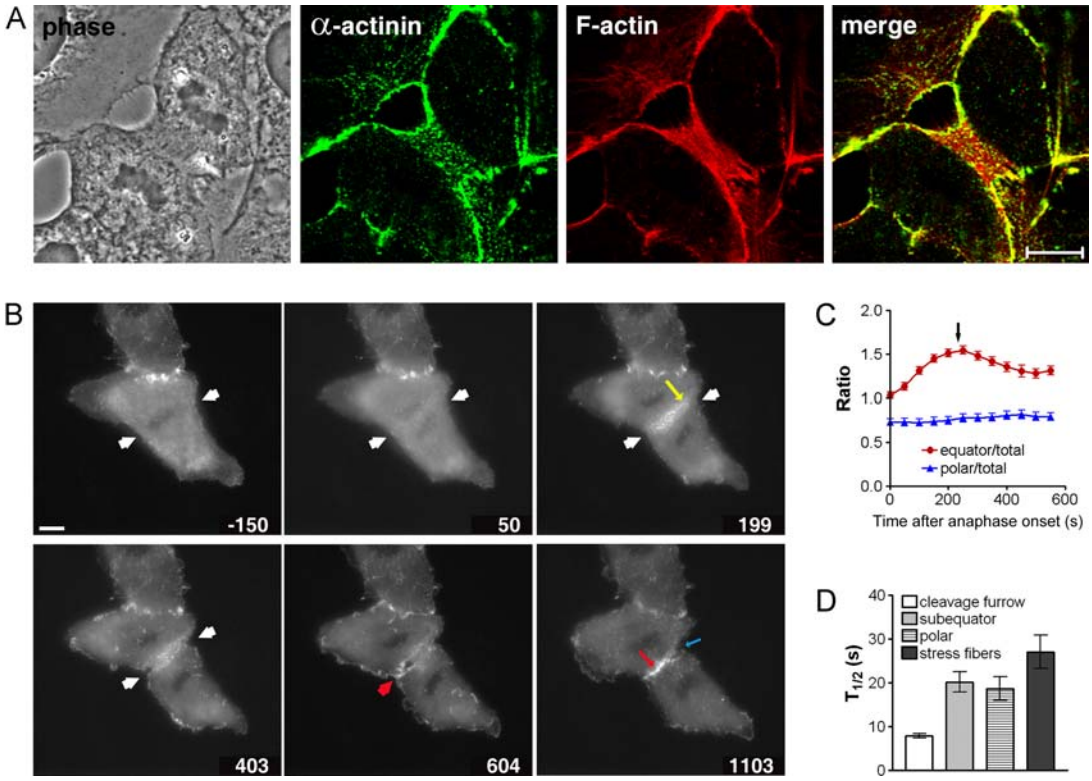

Figure 1. Dynamics of α-Actinin during Cell Division

(A) Localization of endogenous α-actinin during cytokinesis. Cells were fixed and immunostained with antibodies against α-actinin (green) and rhodamine-phalloidin (red). The scale bar represents 10 μm.

(B) An NRK cell expressing α-actinin-GFP was monitored by fluorescence optics. α-actinin-GFP starts accumulating (yellow arrow) along the cleavage furrow (indicated by white arrows) soon after anaphase onset. During furrow ingression, α-actinin dissipates from the cleavage furrow to the subequatorial region (thick red arrow). Upon completion of cytokinesis, α-actinin-GFP accumulates at the sites of cell-cell contacts (red arrow), although it is hardly present in the midbody (blue arrow). Time elapsed in seconds since anaphase onset is shown at the bottom-right corner of each image. The scale bar represents 10 μm.

(C) Quantification of α-actinin-GFP intensity at the cleavage furrow and polar regions. Zero indicates the time of anaphase onset. The arrow indicates time of furrow initiation. Each value represents mean ± SEM (n = 10).

(D) FRAP analysis of α-actinin-GFP during cytokinesis. NRK cells expressing α-actinin-GFP were bleached at the cleavage furrow (n = 15), subequatorial (7–15 μm from the furrow leading edge) (n = 8), and polar regions (n = 3) during cytokinesis or along the stress fibers (n = 13) during interphase. Scale bars represent mean ± SEM.

present in both muscle and nonmuscle cells, interacting with a large number of molecular partners such as α-catenin, vinculin, integrins, and zyxin, and is found in multiple subcellular regions, including sarcomeric z lines, cell-cell and cell-matrix contact sites, and stress fibers (Otey and Carpen, 2004). Interestingly, it has been shown that increased crosslinking of actin filaments by α-actinin inhibits myosin-based contractions in vitro (Janson et al., 1992). Moreover, in the presence of α-actinin, a member of the ADF/cofilin family named actophorin promotes bundling of actin filaments in vitro (Maciver et al., 1991), presumably by limited disruption of the cross-linked network. These observations raise a possibility that modulation of the actin-filaments network by α-actinin might regulate actomyosin contractility and actin bundle assembly during cytokinesis. Although a previous study has indicated a role of α-actinin in cytokinesis of fission yeasts (Wu et al., 2001), little is known about its precise function in relation to cortical contraction.

In the present study, we have dissected the function of α-actinin during cytokinesis of mammalian cells. Our observations strongly suggest that cytokinesis requires the remodeling of actin filaments by α-actinin. We also suggest that cytokinetic ingression requires remodeling rather than the accumulation of actin filaments.

RESULTS

Dynamics of α-Actinin during Cell Division of Mammalian Cells

Consistent with previous reports (Fujiwara et al., 1978; Sanger et al., 1987), endogenous α-actinin primarily accumulated at the equatorial region, and colocalized along actin filaments during cytokinesis of normal rat kidney epithelial (NRK) cells (Figure 1A). α-actinin maintained its activity when fused to GFP, as indicated by its ability to rescue defects caused by depletion of endogenous α-actinin (described later) and its localization in fixed

samples mimicking the endogenous protein (data not shown). α-actinin-GFP was used for visualizing the dynamics of α-actinin during anaphase and cytokinesis (Figure 1B and Movie S1). Cells expressing α-actinin-GFP at a low level showed a small number of α-actinin-containing, dot-like structures on the cortex. At approximately 100 s after anaphase onset, α-actinin-GFP started accumulating along the equator as punctuate structures, which developed into a strong equatorial band during early cytokinesis and dissipated subsequently, thereby leaving little trace around the midbody at late cytokinesis. Quantitative analysis indicated that the fluorescent signal reached its peak simultaneously with furrow initiation (Figure 1C, arrow; 235.0 ± 13.0 s after anaphase onset) and steadily decreased during furrow ingression, whereas its intensity remained essentially unchanged in the polar region during cytokinesis (Figure 1C).

To analyze the dynamics of α-actinin in more details, we performed FRAP analysis of α-actinin-GFP (Figure 1D and Figure S1A in the Supplemental Data available with this article online). Whereas the recovery halftime of α-actinin-GFP along the stress fibers in interphase cells was close to 30 s ($t_{1/2}$ = 27.0 ± 3.8 s; Fraley et al., 2005; Hotulainen and Lappalainen, 2006), the halftime was less than 10 s along the equator ($t_{1/2}$ = 7.9 ± 0.5 s). The subequatorial region showed an intermediate mobility ($t_{1/2}$ = 20.1 ± 2.3 s). These results suggest that α-actinin was highly dynamic at the equator during cytokinesis.

Overexpression of α-Actinin Causes an Increase in Equatorial Actin Filaments, Delayed Cytokinesis, and Cytokinesis Failure

In order to analyze the function of α-actinin, we first performed gain-of-function experiments by overexpressing α-actinin-GFP. Greater than 25% of the cells overexpressing α-actinin were multinucleated at 2 days after transfection, whereas approximately 3% of nontransfected cells were multinucleated (Figure 2A), suggesting that overexpression of α-actinin-GFP inhibits cytokinesis. Time-lapse microscopy confirmed that 23% (13/57) of cells overexpressing α-actinin-GFP failed cytokinesis. The relative amount of α-actinin in cells expressing α-actinin-GFP was estimated by the intensity of immunofluorescence staining. The total amount of α-actinin was increased 4- to 5-fold in cells that had failed cytokinesis, whereas cells with ~2-fold overexpression of α-actinin-GFP had divided normally, suggesting that the cytokinetic defect in cells overexpressing α-actinin-GFP is dependent on its expression level.

In cells that overexpressed α-actinin at high level and that failed cytokinesis (Figure 2C and Movie S2), no apparent defects in spindle positioning or chromosome congression were observed. The failure typically involved slowing of ingression and regression on one side of the furrow, after an apparently symmetric initial ingression. Ingression progressed extremely slowly, lasting for approximately 50 min, while the nuclear envelope formed normally. Eventually, the furrow regressed without forming the midbody, resulting in the formation of a binucleated cell. Corresponding fluorescence images of α-actinin-GFP showed that α-actinin-GFP accumulated strongly along the equator (Figure 2C, blue arrow). In contrast, in control nontransfected cells, furrow ingression typically initiated soon after chromosome separation and progressed from both sides of the equator, and the midbody formed at ~16 min after anaphase onset (Figure 2B and Movie S3).

Because α-actinin-GFP is an actin crosslinking protein, we examined the effects of overexpression of α-actinin-GFP on actin-filament organization by using rhodamine-phalloidin. We detected a significant increase in the density of actin filaments not only along the equator but also throughout the cell cortex, in cells overexpressing α-actinin-GFP compared to control cells (Figures 3A, 3B, and 4C). Overexpression of the truncated α-actinin protein lacking the ability to crosslink actin filaments (the actin-binding domain; ABD) fused to GFP had no effect on the density of actin filaments along the equator, although ABD-GFP was localized to the cleavage furrow (Figures 3C and 3D). Moreover, there was no significant difference in the frequency of multinucleation between cells overexpressing ABD-GFP (3.1% ± 0.2%, n = 356) and control nontransfected cells (2.9% ± 0.4%, n = 369). These results suggest that extensive crosslinking of actin filaments by overexpression of α-actinin leads to increased density of actin filaments, thereby causing cytokinesis failure.

To determine whether overexpression of α-actinin affects actin dynamics along the equator, we performed FRAP analysis of GFP-actin in cells overexpressing α-actinin fused to Cherry fluorescent protein (CherryFP), which induced similar effects and localization pattern as overexpression of α-actinin-GFP (Figure S2). FRAP showed that GFP-actin turned over more slowly in α-actinin-CherryFP overexpressing cells that showed delayed cytokinesis ($t_{1/2}$ = 38.1 ± 5.4 s) compared to control cells ($t_{1/2}$ = 16.9 ± 1.8 s; Guha et al., 2005) and to cells with a low level of α-actinin-CherryFP ($t_{1/2}$ = 16.1 ± 1.6 s) (Figures 3E and 3F and Figure S1B). Overexpression of α-actinin-GFP had no significant effect on the organization of myosin II, which was organized as punctate structures predominantly along the equator of both control cells and cells overexpressing α-actinin-GFP, during cytokinesis (Figures 4A and 4B). These results indicate that overexpression of α-actinin-GFP inhibits actin turnover and causes the accumulation of actin filaments along the equator, without affecting myosin II organization.

In addition to affecting equatorial cortical dynamics, overexpression of α-actinin-GFP may affect cell-substrate adhesion during cytokinesis, and this may in turn affect cytokinesis. Although the failure in cytokinesis cannot be easily explained by a failure in cell rounding, because α-actinin-GFP-overexpressing cells with both larger and normal size showed cytokinesis failure (Figure 2D), we noticed an increase in vinculin plaques throughout the cortex and particularly along the equator with no effect on its protein level, whereas control cells hardly showed any vinculin plaques during division (Figure 4C).

To determine whether overexpression of α-actinin-GFP affects cell rigidity, which may cause cytokinetic defects,

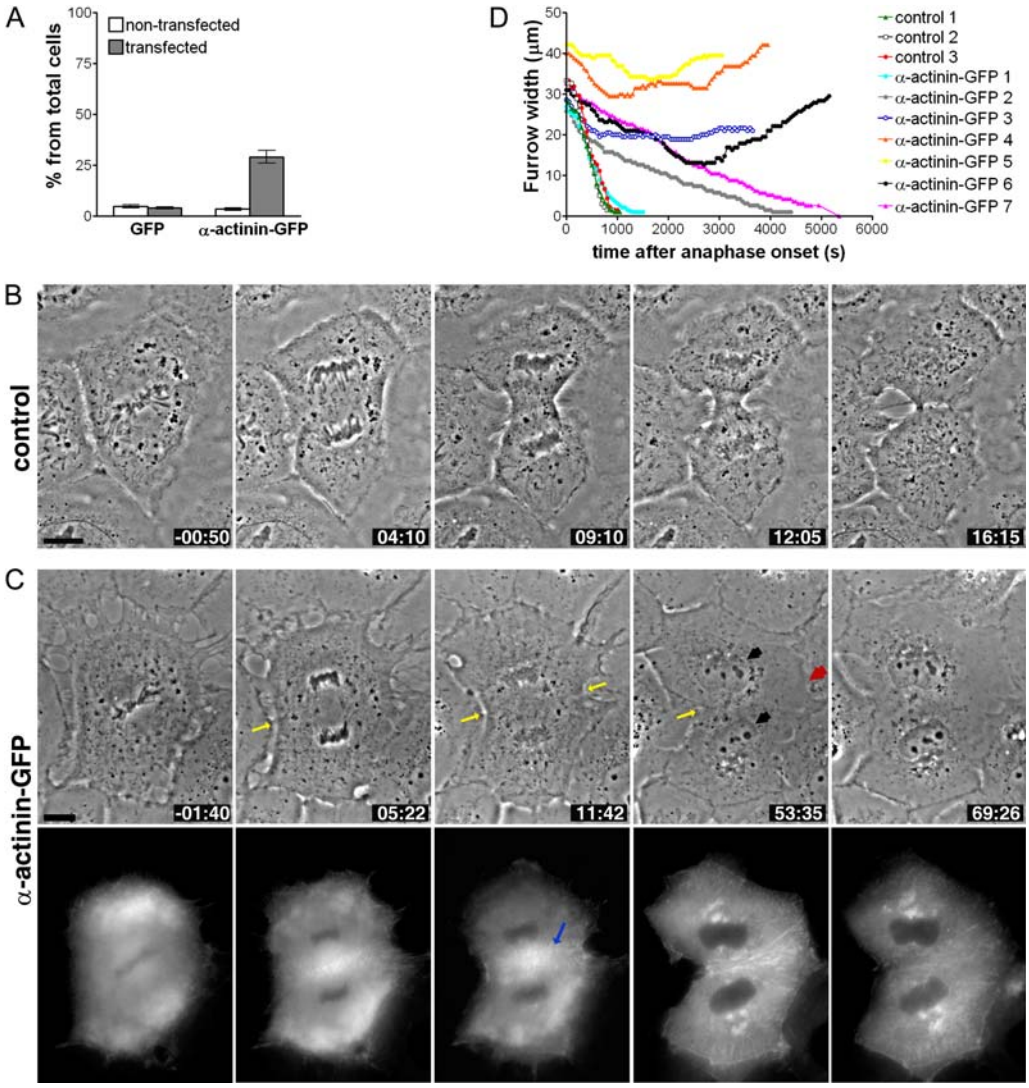

Figure 2. Overexpression of α-Actinin Causes Delayed Cytokinesis and Cytokinesis Failure

(A) Frequency of multinucleation in cells transfected with GFP (n = 273), α-actinin-GFP (n = 361), or nontransfected neighboring cells (n = 452 and n = 1161, accordingly). Scale bars represent mean ± SEM. A control NRK cell (B) or an NRK cell overexpressing α-actinin-GFP at a high level (C) was monitored by time-lapse phase and fluorescence optics. Time elapsed in minutes and seconds after anaphase onset is shown at the bottom-right corner. The initially symmetric furrow regresses on one side of the equator (red arrow). Furrow progression continues even after the furrow regressed from one side of the equator (yellow arrows). During furrow ingression, the nuclear envelope forms normally (black arrows). α-actinin-GFP strongly accumulates along the equator (blue arrow). The scale bar represents 10 μm.

(D) Plots of furrow width over time after anaphase onset. The furrow width was monitored for seven different cells overexpressing α-actinin-GFP and for three representative control cells. Cells shown in Figures 1B, 2C, and 2B are plotted under the name of α-actinin-GFP 1, α-actinin-GFP 4, and control 1, respectively.

we brought a thin glass needle to the side of an early mitotic cell overexpressing α-actinin-GFP or a control cell and moved it toward the center of the cell in 5 μm increments. Images of cells and needles allowed us to calculate the relative cell rigidity. The apparent rigidity of cells overexpressing α-actinin-GFP was slightly increased, compared to that of control cells (Figure 4D and Figure S3), although the difference was not statistically significant ($p = 0.08$). However, even though the cells remained attached to the substrate during probing, we cannot rule out the possibility that the measurements were also affected by altered cell adhesion, which may mask differences in cortical rigidity.

Depletion of α-Actinin Causes Global Decrease in Cortical Actin Filaments, Accelerated Cytokinesis, and Ectopic Furrowing

To determine the effect of disruption of α-actinin-mediated cortical actin crosslinking, we first performed local inactivation of α-actinin at the equator by using chromophore-assisted laser inactivation (CALI), which had been used successfully for inactivating α-actinin in interphase

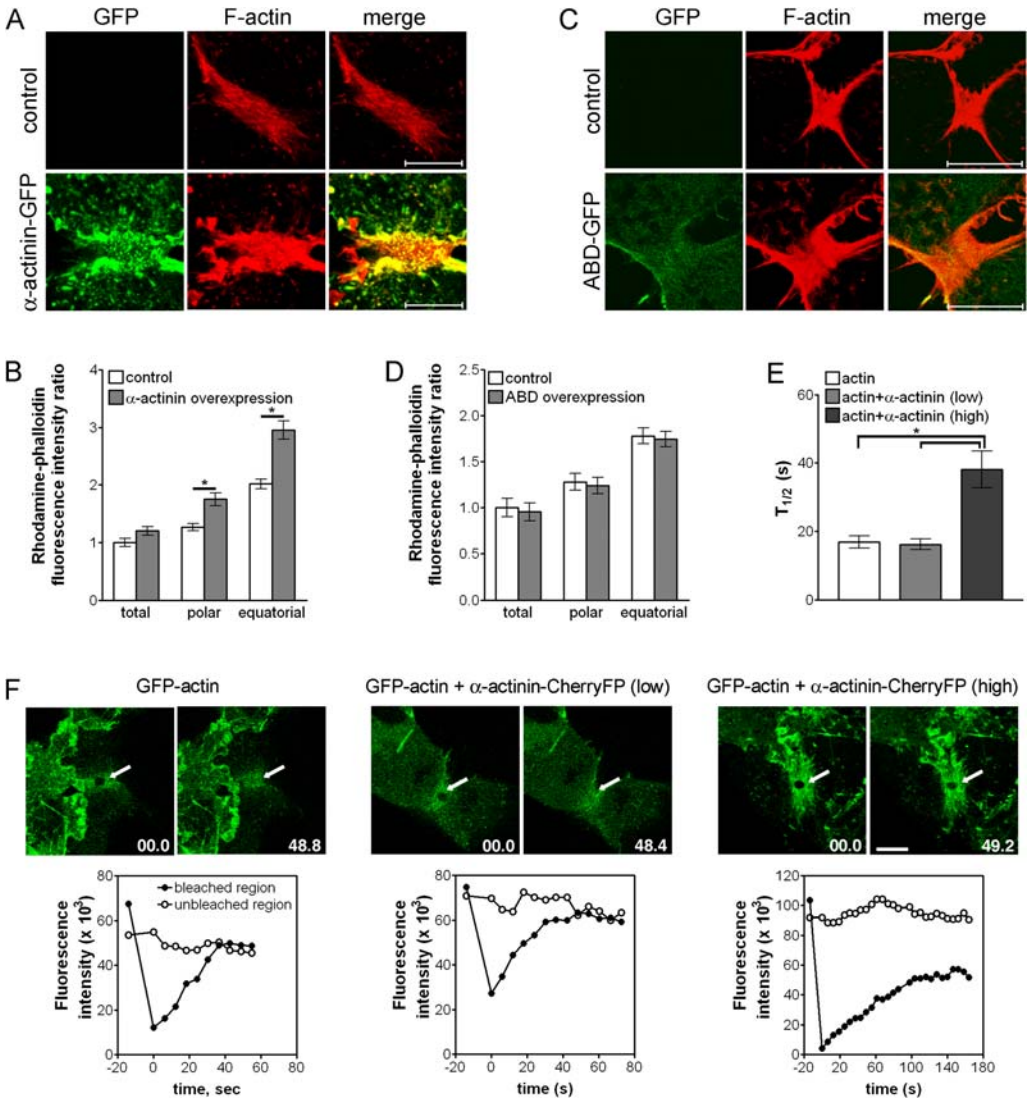

Figure 3. Overexpression of α-Actinin Causes an Increase in the Accumulation of Actin Filaments by Inhibition of Actin Turnover

(A) NRK cells transiently transfected with α-actinin-GFP or control nontransfected cells were fixed and stained with rhodamine-phalloidin (red). Scale bars represent 10 μm. Note that whole-cell images are shown in Figure 4C.

(B) Quantification of F-actin fluorescence intensity in whole cells and at both the equatorial and polar regions of control cells (n = 27) and in cells overexpressing α-actinin-GFP (n = 14) during cytokinesis. Error bars represent mean ± SEM; *p < 0.0001.

(C) NRK cells transiently transfected with ABD-GFP or control nontransfected cells were fixed and stained with rhodamine-phalloidin (red). Scale bars represent 10 μm.

(D) Quantification of F-actin fluorescence intensity in whole cells and at both the equatorial and polar regions of control cells (n = 9) and in cells overexpressing ABD-GFP (n = 10) during cytokinesis. Error bars represent mean ± SEM.

(E) Rate of FRAP for GFP-actin. Error bars represent mean ± SEM, *p < 0.0005.

(F) FRAP analysis of GFP-actin in cells overexpressing α-actinin-CherryFP during cytokinesis. Cells expressing GFP-actin (n = 11), cells expressing both GFP-actin and α-actinin-Cherry at low level and showing normal cytokinesis (n = 13), or cells expressing both GFP-actin and α-actinin-Cherry at high level and showing delayed cytokinesis (n = 5) were bleached in the indicated region (arrows) along the equator. The scale bar represents 10 μm.

cells (Rajfur et al., 2002). CALI on one side of the equator induced a slightly deeper and wider furrow on the irradiated side than the nonirradiated side in approximately 60% of the cells (7/12) (Figure 5A, arrows), whereas such a furrow was rarely observed in control experiments (Figures 5A and 5B). This suggests that weakening of the cortical actin network by local inactivation of α-actinin might facilitate ingression. However, the effect of CALI is expected to be weak and transient because of the rapid exchange of α-actinin along the equator as indicated by FRAP analysis (Figure 1D).

Next, we used the RNA interference (RNAi) technique to deplete α-actinin globally from the cell. Cells microinjected with either of two different siRNAs directed against

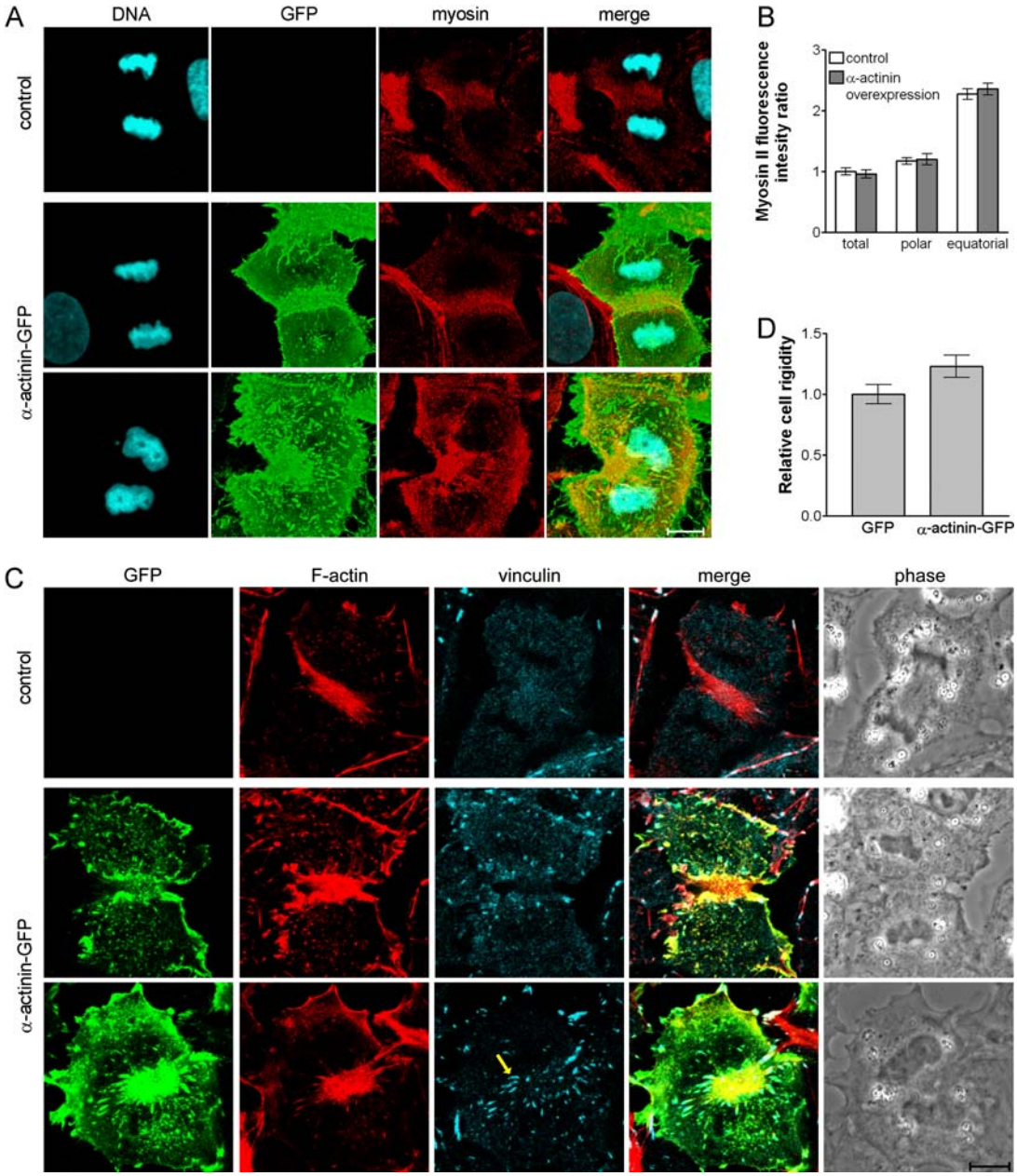

Figure 4. Overexpression of α-Actinin Has No Significant Effect on Myosin II Organization but Induces Precocious Formation of Focal Adhesions during Cytokinesis

(A) NRK cells transiently transfected with α-actinin-GFP (green) or control nontransfected NRK cells were stained with antibodies against myosin II (red) and Hoechst 33258 (blue). Three-dimensional reconstructed images are presented. The scale bar represents 10 μm.

(B) Quantification of myosin II fluorescence intensity in whole cells and at both the equatorial and polar regions of cells overexpressing α-actinin-GFP (n = 10) compared with control cells (n = 19). Error bars represent mean ± SEM.

(C) NRK cells transiently transfected with α-actinin-GFP or control nontransfected cells were fixed and stained with rhodamine-phalloidin (red) and antibodies against vinculin (blue). In cells that overexpressed α-actinin-GFP and that failed cytokinesis, vinculin plaques are observed along the equator (arrow). The scale bar represents 10 μm.

(D) Comparison of relative rigidity of cells overexpressing GFP with that of cells overexpressing α-actinin-GFP. The graph shows the ratio of mean rigidity of cells expressing GFP over that of cells overexpressing α-actinin-GFP. Error bars represent mean ± SEM.

α-actinin (siRNA-1 and 2) showed ~70% reduction of α-actinin level, whereas those injected with a scrambled siRNA showed normal α-actinin distribution and level (Figures S4A and S4B).

Global depletion of α-actinin caused severe defects in the integrity of the cortical actin network during cell division. In approximately 40% of cells depleted of α-actinin, the equatorial cortex suddenly and quickly collapsed

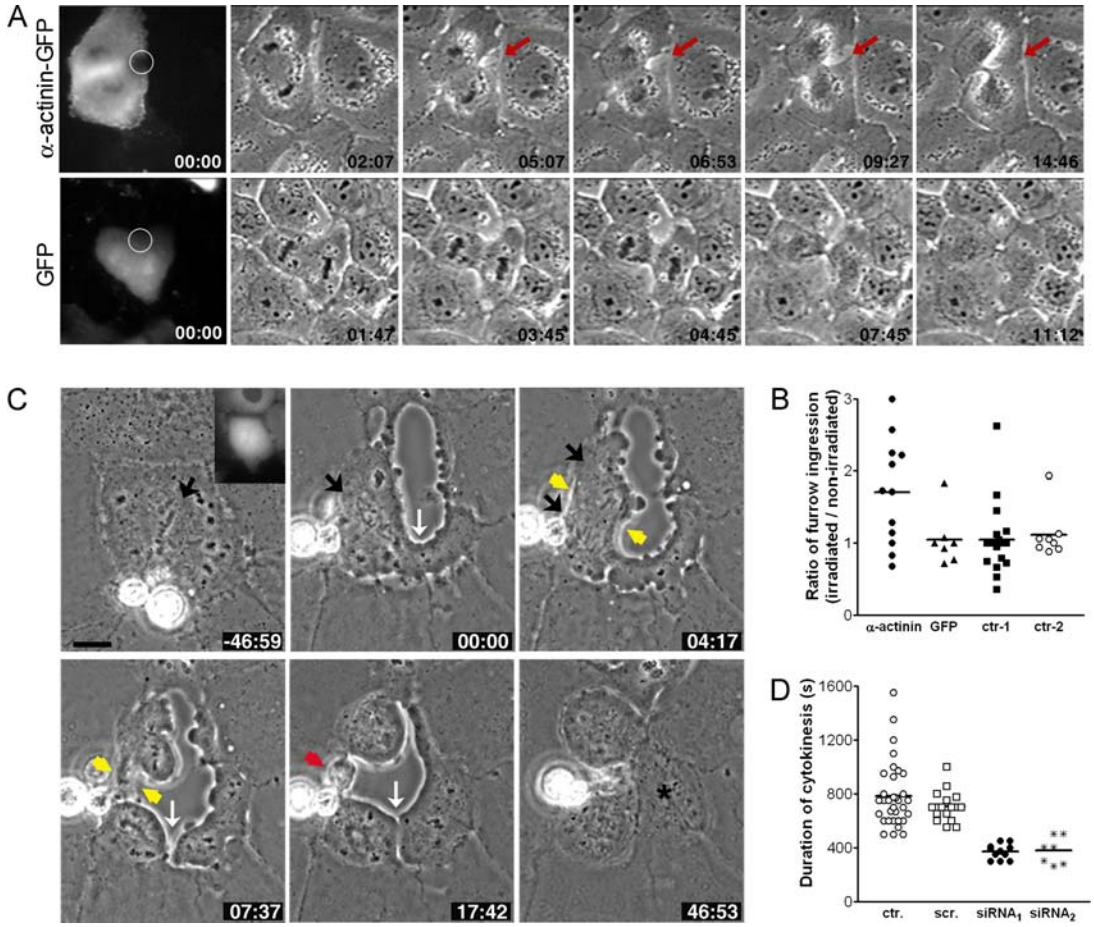

Figure 5. Deactivation or Depletion of α-Actinin Induces Accelerated Cytokinesis

(A) One side of the equatorial region of a dividing NRK cell expressing α-actinin-GFP (top) or GFP only (bottom) was irradiated by a laser beam and monitored by time-lapse phase-contrast optics.

(B) Ratio of furrow ingression between the laser-irradiated side and the nonirradiated side of the equator in cells expressing α-actinin-GFP (n = 12), cells expressing GFP alone (n = 7), and nontransfected cells with (n = 18; control 1) or without (n = 8; control 2) laser irradiation. Bars represent mean values.

(C) Phase-contrast time-lapse images of NRK cells microinjected with siRNA against α-actinin during cell division. Time elapsed in minutes and seconds since anaphase onset is shown at the bottom-right corner of each image. Chromosome congression and separation occur normally (black arrows). However, precocious cortical ingression is induced before anaphase (white arrow), and furrow ingression is accelerated (yellow arrows). Moreover, cytokinesis also occurs outside the equator (white arrow), producing an anuclear fragment of cytoplasm (asterisk). Scale bar represents 10 μm.

(D) Average duration of cytokinesis in control cells or cells depleted of α-actinin. Duration of cytokinesis is ~400 s in cells microinjected with siRNA-1 (n = 11) and siRNA-2 (n = 7) that showed accelerated cytokinesis, whereas it is 700~800 s in noninjected cells (n = 35) and cells microinjected with scrambled siRNA (n = 17). Bars represent mean values.

(Table 1; Figure 5C and Movie S5). In addition, in some cells, an abnormal midbody was formed (Figure 5C, red arrow), and the formation of interphase morphology was delayed. The average duration of cytokinesis in cells that were depleted of α-actinin and that showed rapid furrow ingression was approximately 400 s, as compared to 700–800 s in control noninjected cells and cells microinjected with scrambled siRNA (Figure 5D). Because rapid furrow ingression was concomitant with collapse of the equatorial cortex, we frequently failed to observe midbody formation, which was used as an indication of cytokinesis completion in control cells. Thus, the duration of cytokinesis in the α-actinin-depleted cells that showed rapid furrowing probably represented a slight overestimate because it was measured from the initiation of cytokinesis to the clear formation of two daughter cells.

Surprisingly, we occasionally observed precocious cortical ingression before anaphase onset in approximately 10% of cells depleted of α-actinin (Table 1), although chromosome congression and separation was normal (Figure 5C and Movie S5). Moreover, in some α-actinin-depleted cells, furrow ingression occurred both along and outside the equator after chromosome separation, thereby producing anuclear cell fragments (Figure 5C). Such accelerated cytokinesis and ectopic furrowing were not observed in cells microinjected with scrambled

Table 1. Summary of the Phenotype Observed in Cells Depleted of α-Actinin

		Abnormal Cytokinesis (%)		
			Ectopic Furrowing	
Cells	Normal Cytokinesis (%)	Accelerated Cytokinesis	Total	Before Anaphase Onset
Noninjected (n = 40)	100.0 (n = 40)	-	-	-
Scrambled siRNA (n = 19)	100.0 (n = 19)	-	-	-
siRNA (1) (n = 28)	50.0 (n = 14)	39.3 (n = 11)	17.9 (n = 5)	10.7 (n = 2)
siRNA (2) (n = 19)	52.6 (n = 10)	36.8 (n = 7)	36.8 (n = 7)	10.5 (n = 2)
GFP + siRNA (1) (n = 13)	53.9 (n = 7)	38.5 (n = 5)	23.1 (n = 3)	-
α-actinin-GFP + siRNA (1) (n = 12)	91.7 (n = 11)	8.3 (n = 1)	-	-

NRK cells microinjected with scrambled siRNA, either of two different siRNAs against α-actinin, or the indicated siRNA and empty GFP vector or α-actinin-GFP were monitored by time-lapse phase optics. Percentages of cells that showed each phenotype were calculated from averages of at least three separate experiments.

siRNA (Table 1 and Movie S4). These results suggest that α-actinin is required for the regulation of furrow ingression along the equator and for the prevention of ectopic furrowing during cell division.

Coinjection of siRNA against α-actinin with the α-actinin-GFP expression vector allowed normal cytokinesis in more than 90% of the cells, whereas injection with a mixture of siRNA against α-actinin and the GFP expression vector caused either accelerated cytokinesis or ectopic furrowing or both in almost 50% of the cells (Table 1). These results confirmed (1) that cytokinetic defects observed in cells microinjected with siRNA against α-actinin were due to the depletion of α-actinin and (2) that α-actinin-GFP is functional in vivo.

Because α-actinin is implicated in maintaining cell-cell contacts (Otey and Carpen, 2004), depletion of α-actinin may weaken cell-cell contacts, which may in turn induce accelerated cytokinesis and ectopic furrowing. However, we found that isolated cells depleted of α-actinin also had ectopic furrowing and accelerated cytokinesis (Figure S5), and these findings argued against an induced effect of disrupted cell-cell contacts.

We next examined the effects of depletion of α-actinin on actin-filament organization. A reduced density of actin filaments was detected throughout the cortex of cells depleted of α-actinin compared to that of control cells (Figure 6A), and the total level of actin filaments also decreased slightly (Figure 6B). In contrast, depletion of α-actinin had no effect on either the organization (Figure 6C) or total amount of myosin II (Figure 6D), suggesting that crosslinking of actin filaments by α-actinin did not directly regulate myosin II.

Because myosin II is essential for cytokinesis, we examined whether accelerated cytokinesis and ectopic furrowing induced by depletion of α-actinin require myosin II activity. Blebbistatin, a known inhibitor for myosin II (Straight et al., 2003), was applied to cells microinjected with siRNA against α-actinin. Although DMSO treatment had no effects on accelerated cytokinesis and ectopic furrowing in cells depleted of α-actinin (data not shown), no furrows were detected in cells depleted of α-actinin and treated with blebbistatin (n = 23; Figure 6E) even after cells entered late anaphase (compare with the cells in Figures 6A and 6C). Thus, as for normal furrows, myosin II activity is required for accelerated cytokinesis and ectopic furrowing. To further analyze the relationship between α-actinin and myosin II, we tested whether myosin II affects α-actinin turnover by FRAP analysis of α-actinin-GFP in cells treated with blebbistatin (Figures 6F and Figures S1C and S6). α-actinin-GFP recovers from photobleaching more slowly in cells treated with blebbistatin ($t_{1/2}$ = 29.5 ± 4.5 s) than in control cells treated with DMSO ($t_{1/2}$ = 9.2 ± 0.9 s), showing that myosin II influences the dynamics of α-actinin.

DISCUSSION

Functions of α-Actinin along and outside the Equator

Depletion of α-actinin induced ectopic furrowing even before anaphase onset (Figure 5), suggesting that inward forces are present not only along the equator (Rappaport, 1967) but also on the entire cortex from the early stage of mitosis and that furrow ingression requires remodeling rather than accumulation of actin filaments. This argues against the simplest version of the contractile-ring hypothesis (Schroeder, 1968; Satterwhite and Pollard, 1992; Wang, 2005) and suggests that crosslinking of actin filaments by α-actinin is required for resisting global inward forces, possibly increasing cortical rigidity, outside the equator or before the onset of cytokinesis.

Overexpression of α-actinin slowed down cortical ingression, whereas deactivation or depletion of α-actinin induced rapid furrow ingression, suggesting that α-actinin at the equator regulates furrow-ingression speed after cytokinesis initiates. Although we cannot rule out the possibility that precocious formation of focal adhesions suppressed furrow ingression in cells overexpressing α-actinin, inhibition of actin disassembly and actomyosin-based cortical contraction is most likely to be responsible for the delay in ingression. In addition, disruption of cell-cell or cell-substrate contacts cannot easily explain the precocious ingression caused by the depletion of α-actinin. Finally, the local inactivation experiment supports a direct role of α-actinin at the furrow.

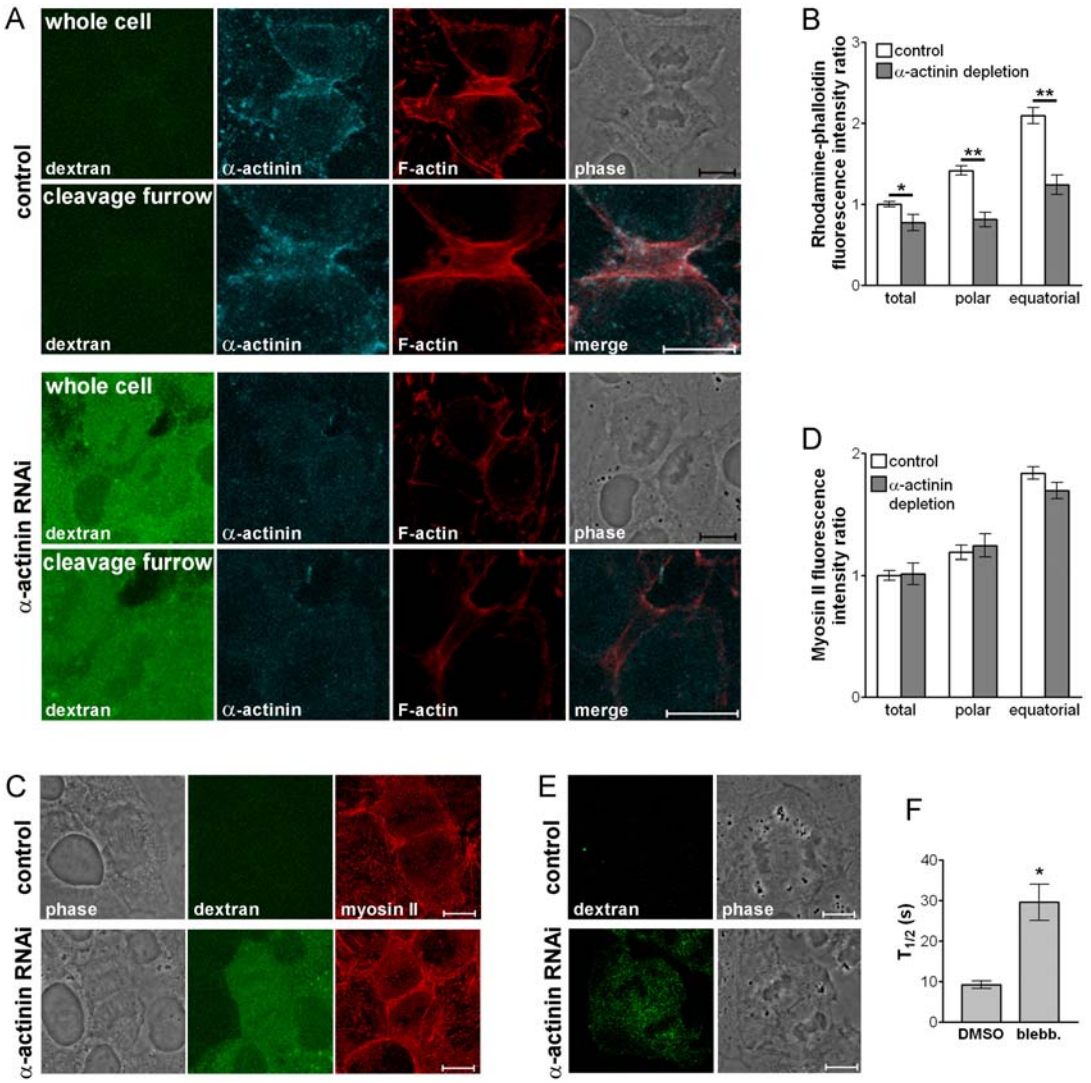

Figure 6. Depletion of α-Actinin Causes a Decrease in the Density of Actin Filaments throughout the Cortex with No Effect on Myosin II

(A) NRK cells microinjected with or without siRNA against α-actinin diluted in fluorescent dextran (green) were fixed and stained with rhodamine-phalloidin (red) and antibodies against α-actinin (blue). Three-dimensional reconstructed images of actin filaments are shown. The scale bar represents 10 μm.

(B) Quantification of actin filaments' fluorescence intensity in whole cells and at both the equatorial and the polar regions of cells depleted of α-actinin (n = 9) compared with control cells (n = 13). Error bars represent mean ± SEM; *p < 0.05, **p < 0.0001.

(C) NRK cells microinjected with or without siRNA against α-actinin diluted in fluorescent dextran (green) were fixed and stained with antibodies against myosin II (red). Three-dimensional reconstructed images are presented. Scale bars represent 10 μm.

(D) Quantification of myosin II fluorescence intensity at both the equatorial and polar regions of cells depleted of α-actinin (n = 7) compared with control cells (n = 15). Error bars represent mean ± SEM.

(E) NRK cells microinjected with or without siRNA treated with blebbistatin. Scale bars represent 10 μm.

(F) FRAP analysis of α-actinin-GFP during cytokinesis of cells treated with blebbistatin. NRK cells expressing α-actinin-GFP were treated with blebbistatin (n = 10) or DMSO (n = 16) and bleached at the equatorial region. Error bars represent mean ± SEM; *p < 0.0001.

Comparison of the Function of α-Actinin in Cytokinesis between Fission Yeast and Mammalian Cells

The α-actinin-like protein Ain1p has been implicated in cytokinesis of fission yeasts (Wu et al., 2001). Overexpression of Ain1p caused either mispositioned or disorganized actin rings or both, whereas deletion of the *Ain1* gene caused formation of an abnormal, thin actin ring under certain stress conditions, suggesting that Ain1p is involved in the formation of equatorial actin ring. Ain1p has only two spectrin-like domains instead of four in mammalian cells. Hence, Ain1p may form actin bundles instead of a network caused by conventional α-actinin, which is possibly responsible for the tightly packed actin ring in

yeast (Wu et al., 2001). In contrast to the short length of Ain1p, conventional α-actinin may crosslink actin filaments loosely at the equator, where an apparent ring structure is hardly detected during cytokinesis of mammalian cells under some conditions (Fishkind and Wang, 1993).

The number of multinucleated yeast cells increased not only upon overexpression of the Ain1p protein but also in Ain1 deletion mutants (Wu et al., 2001), suggesting that Ain1p helps proper formation of the actin ring rather than remodeling of actin filaments. This differs from our results in mammalian cells, in which furrow ingression speeds up and even ectopic furrows are formed by loss of α-actinin. Thus, although the cytokinetic components are well conserved between fission yeast and mammalian cells, the regulation of furrow ingression is likely to depend on the organization of the contractile ring.

Regulation of the Cortical Actin Network by α-Actinin during Cytokinesis

How does α-actinin regulate the change of cell shape (i.e., furrow ingression) along the equator? A previous report demonstrated that, at high rates of deformation, the actin network crosslinked by α-actinin is stiffer than actin filaments alone, whereas at low rates of deformation, there is no effect on the mechanical properties of the crosslinked actin network (Sato et al., 1987). Assuming that α-actinin forms dynamic crosslinks between actin filaments, the actin network may deform easily under a slowly provided force as seen in cytokinesis of animal cells (Rappaport, 1967). In addition, an important function of α-actinin might be to suppress rapid, random shape changes due to local fluctuations in motor activities.

A separate study showed that increasing the concentration of α-actinin relative to actin causes stiffening of the actin gel and makes the gel more solid-like regardless of the deformation rate (Tseng and Wirtz, 2001). Conversely, decreases in α-actinin causes the gel to become more liquid-like. This may explain the inhibition of ingression upon overexpression of α-actinin and the poorly regulated ingression upon depletion of α-actinin. The behavior of the cortical gel is probably also affected by myosin II forces, which may rupture the association between actin and α-actinin and cause "strain softening" (Heidemann and Wirtz, 2004). Therefore, under normal conditions, accumulation of α-actinin at the equator is likely to cause an increase in viscoelasticity of the isotropic actin network before furrow initiation. However, subsequent increases in myosin-driven forces might promote not only contraction but also release of α-actinin from the equator, thereby causing a decrease in cortical viscoelasticity and rearrangement of the crosslinked actin network, leading to cell shape change (i.e., ingression of the furrow).

Our observations elucidate the regulation of furrow ingression by α-actinin. The overall regulating mechanism of cytokinesis, however, is likely to be more complex. The effects of actin-associated proteins on the mechanical properties of the actin network during cytokinesis have been studied in *Dictyostelium* (Reichl et al., 2005). In *Dictyostelium*, furrow contractility is multiphasic, and both the global and the equatorial actin network, regulated differentially by various actin crosslinkers, myosin II, and a small GTPase, have distinct and important roles in furrow ingression (Girard et al., 2004; Zhang and Robinson, 2005; Octtaviani et al., 2006). Compared with *Dictyostelium*, mammalian cell lines such as NRK cells do not undergo as dramatic a change in morphology during cytokinesis. In addition, these cells do not form a cylinder-shaped cleavage furrow as *Dictyostelium* does (Zhang and Robinson, 2005). Therefore, the mechanism for the regulation of furrow ingression in mammalian cells may be different from that of *Dictyostelium*. However, because many other proteins are involved in cytokinesis of mammalian cells, it is important to elucidate how they function and interact spatiotemporally in order to regulate furrow ingression during cytokinesis.

EXPERIMENTAL PROCEDURES

Cell Culture, Microscopy, and Image Processing

NRK cells (NRK-52E; ATCC) were maintained in Kaighn's modified F12 (F12K) medium supplemented with 10% FBS (BioWest), 100 U/ml penicillin, and 100 μg/ml streptomycin. Cells were grown on glass chamber dishes as previously described (McKenna and Wang, 1989). For live-cell imaging, the cells were maintained at 37°C in a custom-made incubator built on top of an Axiovert 200 M inverted microscope (Carl Zeiss) and viewed with a 100×, NA 1.30, Plan-NEOFLUAR lens. All images were acquired with a cooled charge-coupled device camera (CoolSNAP$_{HQ}$, Roper Scientific) and processed with MetaView imaging software (Universal Imaging). Immunofluorescence staining was analyzed with a LSM 510 Meta confocal microscope system (100×, NA 1.25 Achroplan lens, 100×, NA 1.4 Plan-Apochromat lens, or 63×, NA 1.4 Plan Apochromat lens; Carl Zeiss).

Plasmids

α-actinin-GFP (α-actinin-4-GFP; Gonzalez et al., 2001) was a generous gift from Dr. Carol Otey (University of North Carolina, USA). GFP-actin and empty pEGFP vectors were from BD Biosciences Clontech, whereas pmax GFP was obtained from Amaxa. We constructed α-actinin-CherryFP with α-actinin-GFP by replacing a DNA fragment encoding GFP with that encoding CherryFP. The actin-binding domain (ABD) of α-actinin (encoding amino acids 28–292) was amplified by PCR with α-actinin-GFP as a template and subcloned into pEGFP-N1.

Transfection and RNA Interference

NRK cells grown on glass chamber dishes were transiently transfected with 1.6 μg of plasmids with Superfect reagent (QIAGEN) in accordance with the manufacturer's instruction. After 2 hr of incubation, the medium containing the DNA-Superfect complex was replaced with F12K medium containing 10% FBS, and the cells were incubated for an additional 48 hr. Alternatively, cells were transfected with 0.3 μg of the plasmids with Effectene reagent diluted in F12K medium containing 1% FBS for 8–12 hr. The DNA-Effectene complex was replaced with the F12K medium containing 10% FBS, and the cells were cultured for an additional 24-48 hr.

Two different Silencer Predesigned siRNA duplexes against rat α-actinin-4 and a Silencer Negative Control #1 siRNA duplex were purchased from Ambion. Each siRNA was diluted to the final concentration of 500 nM in HEK buffer (20 mM HEPES, 10 mM KCl [pH 7.7]) with 5 mg/ml lysine fixable 70,000 MW fluorescein dextran (Molecular Probes) and then microinjected into the cells with custom-drawn glass needles and a FemtoJet pressure control system (Eppendorf). The cells microinjected with each siRNA were cultured for 72 hr. For rescue experiments, cells were microinjected with siRNA (500 nM) together

with 300 μg/ml of either empty GFP vector or α-actinin-GFP and cultured for 72 hr.

Fluorescence Recovery after Photobleaching

NRK cells were transiently transfected with α-actinin-GFP, GFP-actin, or both GFP-actin and α-actinin-CherryFP with Effectene transfection reagent as described above. FRAP was performed with a Zeiss Meta 510 confocal microscope, with a 100×, NA 1.25 Achroplan objective. Bleaching of the marked region was carried out at 100% laser power with 150 iterations. Time-lapse images were acquired at every 6 s interval. Fluorescence recovery was analyzed with MetaView.

Chromophore-Assisted Laser Inactivation

NRK cells were transiently transfected with α-actinin-GFP or pmax GFP plasmid with Effectene transfection reagent as described above. Cells expressing α-actinin-GFP at a low level were selected for CALI. Cells were irradiated for 200 ms with a focused beam from a Lexel Model 94 argon ion laser (488 nm, 500 mW of power at the laser head), with a 100×, NA 1.30 Plan Neofluar lens, mounted on a Zeiss Axiovert Inverted microscope. The laser beam was first applied after anaphase onset but before initiation of ingression to one side of the equator. As ingression progressed, the same region was irradiated for an additional three to four times. Fluorescence and phase-contrast images were acquired with a cooled charge-coupled device camera (ST133 controller and CCD57 chip; Roper Scientific) and processed with custom software for background subtraction.

Immunofluorescence

Cells were briefly rinsed with warm PBS and fixed with 4% paraformaldehyde (EM Sciences) in warm PBS for 10 min. They were then rinsed thoroughly in PBS and permeabilized by incubation with 0.2% Triton X-100 for 5 min. Fixed cells were rinsed with PBS, blocked for 30 min with 3% BSA (Boehringer Mannheim) in PBS (PBS/BSA), and incubated with primary antibodies diluted in PBS/BSA for 1 hr at 37°C. Primary antibodies were diluted as follows: 1:200 anti-α-actinin antibodies (ImmunoGlobe), 1:100 anti-vinculin antibodies (Upstate), and 1:500 anti-myosin II (A + B) antibodies. After three 10 min rinses with PBS/BSA, cells were incubated with goat anti-mouse (vinculin) or anti-rabbit (α-actinin and myosin) antibodies conjugated with Alexa Fluor 488, Alexa Fluor 546, or Alexa Fluor 647 (Molecular Probes) at a dilution of 1:300.

For observing actin filaments, fixed cells were stained with rhodamine-phalloidin (Molecular Probes) at a dilution of 1:300 for 1 hr at 37°C.

For locating the chromosomes, cells were incubated with 10 μg/ml Hoechst 33258 (Sigma-Aldrich) for 10 min at room temperature.

Quantification of Fluorescence Signals

Expression level of α-actinin-GFP was estimated by quantitative immunofluorescence.

For analysis of α-actinin-GFP dynamics during cytokinesis (Figure 1B), fluorescence intensity of α-actinin-GFP in the entire region of the cleavage furrow, in the polar region with the same width as the cleavage furrow, and in the whole cell was measured.

Fluorescence intensity of actin filaments, myosin II, and vinculin along the equator or near the polar cortex was measured at two different regions (3 × 3 μm^2 for F-actin, myosin II, and vinculin). Graphs representing the quantification of fluorescence intensity (Figures 3B, 3D, 4B, 6B, and 6D) show the ratio of average fluorescence intensity at the indicated region over mean fluorescence intensity of whole control cells.

Drug Treatment

S-(-) isomer of blebbistatin (Toronto Research) was dissolved at 100 mM in 90% DMSO. Cells were incubated with blebbistatin at the final concentration of 100 μM or 0.45% DMSO for 45–90 min prior to FRAP analyses or fixation.

Measurement of Relative Cell Rigidity

Cell rigidity was measured with glass needles with a method modified from that of Maddox and Burridge (2003). In brief, a thin glass needle was brought to the side of a prometaphase or metaphase cell overexpressing GFP or α-actinin-GFP. The needle was moved toward the center of the cell in 5 μm increments with a custom-made micromanipulator, and the position of the tip was measured at each increment from the images. The deformation of the needle, calculated as the difference between needle position and tip position, was then plotted against the deformation of the cell (position of the tip), and the spring constant was determined from the slope as an indicator of cell rigidity. The same needle was used for control cells overexpressing GFP and cells overexpressing α-actinin-GFP, and five to ten cells were analyzed in each experiment. Three independent experiments were performed.

Supplemental Data

Supplemental Data include six figures and five movies and are available with this article online at http://www.developmentalcell.com/cgi/content/full/13/4/554/DC1/.

ACKNOWLEDGMENTS

We would like to thank Dr. Carol Otey (University of North Carolina, USA) for her kind gift of α-actinin-GFP expression vector and Dr. Masayuki Takahashi (Hokkaido University, Japan) for anti-myosin IIA and IIB antibodies. We also thank Adrian Ng and Shyan Huey Low for technical assistance and Dr. Pernille Rørth, Dr. William Chia, Dr. Mohan Balasubramanian, Dr. Snezhana Oliferenko, Dr. Volker Wachtler, and all lab members of the Murata-Hori laboratory for discussions and/or critical reading of the manuscript. This study was supported by intramural funds from the Temasek Life Sciences Laboratory to M.M.-H., and by National Institutes of Health grant GM-32476 to Y.-L.W.

Received: February 20, 2007
Revised: June 12, 2007
Accepted: August 6, 2007
Published: October 9, 2007

REFERENCES

Burton, K., and Taylor, D.L. (1997). Traction forces of cytokinesis measured with optically modified elastic substrata. Nature *385*, 450–454.

Djinovic-Carugo, K., Young, P., Gautel, M., and Saraste, M. (1999). Molecular basis for cross-linking of actin filaments: Structure of the α−actinin rod. Cell *98*, 537–546.

Fishkind, D.J., and Wang, Y.-L. (1993). Orientation and three-dimensinal organization of actin filaments in dividing cultured cells. J. Cell Biol. *123*, 837–848.

Fraley, T.S., Pereira, C.B., Tran, T.C., Singleton, C.A., and Greenwood, J.A. (2005). Phosphoinositide binding regulates α−actinin dynamics. J. Biol. Chem. *280*, 15479–15482.

Fujiwara, K., and Pollard, T.D. (1976). Fluorescent antibody localization of myosin in the cytoplasm, cleavage furrow, and mitotic spindle of human cells. J. Cell Biol. *71*, 848–875.

Fujiwara, K., Porter, M.E., and Pollard, T.D. (1978). Alpha-actinin localization in the cleavage furrow during cytokinesis. J. Cell Biol. *79*, 268–275.

Girard, K.D., Chaney, C., Delannoy, M., Kuo, S.C., and Robinson, D.N. (2004). Dynacortin contributes to cortical viscoelasticity and helps define the shape changes of cytokinesis. EMBO J. *23*, 1536–1546.

Glotzer, M. (2004). Cleavage furrow positioning. J. Cell Biol. *164*, 347–351.

Gonzalez, A.M., Otey, C., Edlund, M., and Jones, C.R. (2001). Interactions of a hemidesmosome component and actinin family members. J. Cell Sci. *114*, 4197–4206.

Guha, M., Zhou, M., and Wang, Y.-L. (2005). Cortical actin turnover during cytokinesis requires myosin II. Curr. Biol. *15*, 732–736.

Gunsalus, K.C., Bonaccorti, S., Williams, E., Verni, F., Gatti, M., and Goldberg, M.L. (1995). Mutations in twinstar, a Drosophila gene encoding a cofilin/ADF homologue, result in defects in centrosome migration and cytokinesis. J. Cell Biol. *131*, 1243–1259.

Heidemann, S.R., and Wirtz, D. (2004). Towards a regional approach to cell mechanics. Trends Cell Biol. *14*, 160–166.

Hotulainen, P., Paunola, E., Vartiainen, M.K., and Lappalainen, P. (2005). Actin-depolymerizing factor and cofilin-1 play overlapping roles in promoting rapid F-actin depolymerization in mammalian non-muscle cells. Mol. Biol. Cell *16*, 649–664.

Hotulainen, P., and Lappalainen, P. (2006). Stress fibres are genereated by two distinct actin assembly mechanisms in motile cells. J. Cell Biol. *173*, 383–394.

Janson, L.W., Sellers, J.R., and Taylor, D.L. (1992). Actin-binding proteins regulate the work performed by myosin II motors on single actin filaments. Cell Motil. Cytoskeleton *122*, 274–280.

Mabuchi, I., Hamaguchi, Y., Kobayashi, T., Hosoya, H., Tsukita, S., and Tsukita, S. (1985). Alpha-actinin from sea urchin eggs: Biochemical properties, interaction with actin, and distribution in the cell during fertilization and cleavage. J. Cell Biol. *100*, 375–383.

Maciver, S.K., Wachsstock, D.H., Schwarz, W.H., and Pollard, T.D. (1991). The actin filament severing protein actophorin promotes the formation of rigid bundles of actin filaments crosslinked with α-actinin. J. Cell Biol. *115*, 1621–1628.

Maddox, A.S., and Burridge, K. (2003). RhoA is required for cortical retraction and rigidity during mitotic cell rounding. J. Cell Biol. *160*, 255–265.

Maddox, A.S., and Oegema, K. (2003). Deconstructing cytokinesis. Nat. Cell Biol. *5*, 773–776.

Maupin, P., and Pollard, T.D. (1986). Arrangement of actin filaments and myosin-like filaments in the contractile ring and of actin-like filaments in the mitotic spindle of dividing HeLa cells. J. Ultrastruct. Mol. Struct. Res. *94*, 92–103.

McKenna, N.M., and Wang, Y.-L. (1989). Culturing cells on the microscope stage. Methods Cell Biol. *29*, 195–205.

Murthy, K., and Wadsworth, P. (2005). Myosin-II-dependent localization and dynamics of F-actin during cytokinesis. Curr. Biol. *15*, 724–731.

Nakano, K., and Mabuchi, I. (2006). Actin-depolymerizing protein Adf1 is required for formation and maintenance of the contractile ring during cytokinesis in fission yeast. Mol. Biol. Cell *17*, 1933–1945.

O'Connell, C., Warner, A., and Wang, Y.-L. (2001). Distinct roles of the equatorial and polar cortices in the cleavage of adherent cells. Curr. Biol. *11*, 702–707.

Octtaviani, E., Effler, J.C., and Robinson, D.N. (2006). Enlazin, a natural fusion of two classes of canonical cytoskeletal proteins, contributes to cytokinesis dynamics. Mol. Biol. Cell *17*, 5275–5286.

Otey, C.A., and Carpen, O. (2004). Alpha-actinin revisited: A fresh look at an old player. Cell Motil. Cytoskeleton *58*, 104–111.

Pelham, R.J., and Chang, F. (2002). Actin dynamics in the contractile ring during cytokinesis in fission yeast. Nature *419*, 82–86.

Rajfur, Z., Roy, P., Otey, C., Romer, L., and Jacobson, K. (2002). Dissecting the link between stress fibres and focal adhesions by CALI with EGFP fusion proteins. Nat. Cell Biol. *4*, 286–293.

Rappaport, R. (1967). Cell division: Direct measurement of maximum tension exerted by furrow of echinoderm eggs. Science *156*, 1241–1243.

Reichl, E.M., Effler, J.C., and Robinson, D.N. (2005). The stress and strain of cytokinesis. Trends Cell Biol. *15*, 200–206.

Sanger, J.M., and Sanger, J.W. (1980). Banding and polarity of actin filaments in interphase and cleaving cells. J. Cell Biol. *86*, 568–575.

Sanger, J.M., Mittal, B., Pochapin, M.B., and Sanger, J.W. (1987). Stress fiber and cleavage furrow formation in living cells microinjected with fluorescently labeled alpha-actinin. Cell Motil. Cytoskeleton *7*, 209–220.

Sato, M., Schwarz, W.H., and Pollard, T.D. (1987). Dependence of the mechanical properties of actin/α-actinin gels on deformation rate. Nature *325*, 828–830.

Satterwhite, L.L., and Pollard, T.D. (1992). Cytokinesis. Curr. Opin. Cell Biol. *4*, 43–52.

Schroeder, T.E. (1968). Cytokinesis: Filaments in the cleavage furrow. Exp. Cell Res. *53*, 272–276.

Somma, M.P., Fasulo, B., Cenci, G., Cundari, E., and Gatti, M. (2002). Molecular dissection of cytokinesis by RNA interference in Drosophila cultured cells. Mol. Cell. Biol. *13*, 2448–2460.

Straight, A.F., Cheung, A., Limouze, J., Chen, I., Westwood, N.J., Sellers, J.R., and Mitchison, T.J. (2003). Dissecting temporal and spatial control of cytokinesis with a myosin II inhibitor. Science *299*, 1743–1747.

Suzuki, A., Goll, D.E., Singh, I., Allen, R.E., Robson, R.M., and Stromer, M.H. (1976). Some properties of purified skeletal muscle α-actinin. J. Biol. Chem. *251*, 6860–6870.

Tseng, Y., and Wirtz, D. (2001). Mechanics and multiple-particle tracking microheterogeneity of alpha-actinin-cross-linked actin filament networks. Biophys. J. *81*, 1643–1656.

Wang, Y.-L. (2005). The mechanism of cortical ingression during early cytokinesis: Thinking beyond the contractile ring hypothesis. Trends Cell Biol. *15*, 581–588.

Wu, J.Q., Bahler, J., and Pringle, J.R. (2001). Roles of a fimbrin and an alpha-actinin-like protein in fission yeast cell polarization and cytokinesis. Mol. Biol. Cell *12*, 1061–1077.

Ylanne, J., Scheffzek, K., Young, P., and Saraste, M. (2001). Crystal structure of the α-actinin rod reveals an extensive torsional twist. Structure *9*, 597–604.

Zhang, W., and Robinson, D.N. (2005). Balance of actively generated contractile and resistive forces controls cytokinesis dynamics. Proc. Natl. Acad. Sci. USA *102*, 7186–7191.